

Numerical Simulations of Exposed Circular Surface of Rolled Homogeneous Armor Steel Plates Subjected to Blast Loadings by Using AUTODYN 2D

Mohd Zaid Othman¹, Lee Choon Yuan¹, Mohd Aidil Mohd Yusop¹, Amir Radzi Ab Ghani², Md Fuad Shah Koslan^{3,1}, Jestin J.¹ & Ahmad Mujahid Ahmad Zaidi^{1,4}

¹ Faculty of Engineering, National Defence University of Malaysia, Kuala Lumpur, Malaysia

² Faculty of Mechanical Engineering, Universiti Teknologi MARA, Shah Alam, Malaysia

³ Royal Malaysian Air Force, Ministry of Defence, Kuala Lumpur, Malaysia

⁴ International College of Automotive (ICAM), Pekan, Pahang, Malaysia

Correspondence: Mohd Zaid Othman, Department of Mechanical Engineering, Faculty of Engineering, National Defence University of Malaysia, Kuala Lumpur, Malaysia, Tel: 6-012-404-5002. E-mail: zaid002@gmail.com

Received: October 28, 2014

Accepted: November 9, 2014

Online Published: January 15, 2015

doi:10.5539/mas.v9n3p216

URL: <http://dx.doi.org/10.5539/mas.v9n3p216>

Abstract

Numerical predictions of responses of rolled homogeneous armour steel plates subjected to spherical trinitrotoluene blast loading plate are presented in this paper. Three simulation cases are modelled using a numerical simulation software, AUTODYN 2D in order to predict the plate deformations under blast loading effects of spherical trinitrotoluene high explosive charge. AUTODYN 2D utilises two dimensional modelling space or axisymmetric modelling space to simulate three dimensional actual experimental tests in order to speed up the computational processing time. Three main geometrical parts namely; air, trinitrotoluene and rolled homogeneous armour steel plate are modelled in AUTODYN 2D utilising the LAGRANGE and EULER element formulations' solvers. Despite the limitations of the two dimensional modelling space utilised in AUTODYN 2D, the simulation results managed to give relatively good agreement (differences in the range of 9.91%-31.25%) with respect to the experimental results from a published paper.

Keywords: blast loading, numerical analysis, AUTODYN 2D, rolled homogeneous armour steel plate

1. Introduction

Terrorist attack has become one of the world major safety concerns nowadays. One of the most recent terrorist attacks was at the Boston marathon event, Boston, United States of America. Explosions from two pressure cooker bombs which sent out blast waves at high pressure killed 3 people and injured 264 people. A pressure cooker bomb is an improvised explosive device (IED) created by inserting explosive material into a pressure cooker and attaching a blasting cap into the cover of the cooker. The bomb can be ignited using simple electronic devices such as a digital watch or alarm clock (New York Daily News, 2014). The literatures on blast loadings scenarios investigated experimentally, analytically and numerically are very well established (K. V. Subramaniam et al., 2009; M. S. Chaffi et al., 2009; Xiang Fang et al., 2011; Yaohua Wang et al., 2011; Md Fuad Shah bin Koslan et al., 2013). When a bomb explodes, high intensity pressures are produced and expanded in a spherical shaped originated from the central point of the explosion to its surrounding (P. D. Smith & J. G. Hetherington, 1994).

Scaled down blast experimental tests have been performed to study the energy absorbing capabilities of 20 liter of water container to absorb blast loading effects of landmine against the undercarriage of armoured vehicles and they found out that the water container could reduce the deformation of square 10 mm thick Grade 350 mild steel plate by as much as 67% (Bornstein et al., 2015). Domex-700 MC circular steel plates have been subjected to repeated blast loads and showed large plastic deformation and large reduction in thickness with tearing phenomena especially at the clamped location (Henchie et al., 2014). They performed experimental and numerical studies i.e. ABAQUS/Explicit finite element analysis software and it was observed that good agreement was achieved by the numerical studies where it gave good predictions of the central deformation and

deformation patterns of the steel plates. Mathematical models to predict the response of fully clamped, circular orthotropic elastic plates subjected to underwater explosion have been successfully developed and gave good correlation with ABAQUS/Explicit finite element analysis software (Schiffer & Tagarielli, 2014). They observed that the layup arrangement played little influence on the blast loading response of composite structure for underwater explosion.

There are several methodologies to investigate the effects of blasts which include experimental tests, mathematical models and computer numerical simulations. However, experimental tests/physical tests pose challenges due to the dangerous and destructive nature of blast events. Strict safety requirements need to be adhered to and they involve a very high cost to conduct. Computer/numerical simulation are one of the safest and efficient ways to substitute the experimental tests. Computer/numerical simulation enable researchers to simulate blast scenarios and obtain valuable outputs in almost any conditions without endangering human lives and properties.

This study will perform numerical simulations to predict the deflections of fully clamped exposed circular surface of rolled homogeneous armour (RHA) plates subjected to sphere-shaped trinitrotoluene (TNT) charge with the appropriate scaling distance. TNT is a chemical explosive with convenient handling properties while RHA is a type of steel used in armoured military vehicles. Numerical simulations using AUTODYN 2D were performed to predict three case studies i.e. the first and final deformations of Case 'A', Case 'B', and Case 'C' from experimental tests (see Table 1) which had been conducted and published (Neuberger et al., 2009) as shown in Figures 1 and 2.

Table 1. The experimental test data for the first and final deflections of the RHA plate subjected to blast loading as conducted by Neuberger and his co-researchers (Neuberger et al., 2009)

Case	W (kg TNT)	R (mm)	Diameter (mm)	Thickness (mm)	First deflection (mm)	Final deflection (mm)
'A'	3.75	200	1000	20	54	7
'B'	8.75	200	1000	20	107	64
'C'	8.75	130	1000	20	165	121

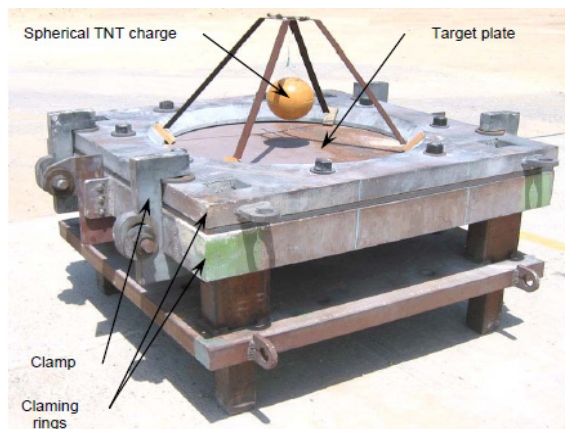


Figure 1. The experimental test apparatus as conducted by Neuberger and his co-researchers (Neuberger et al., 2009)

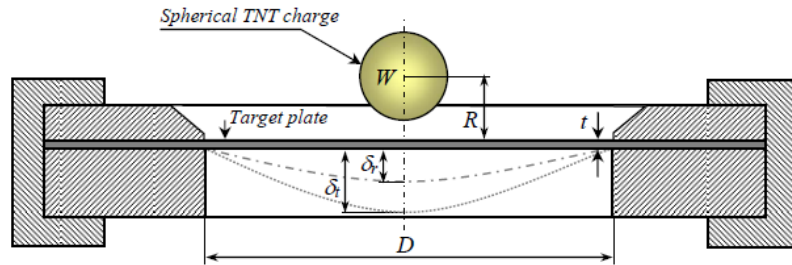


Figure 2. The experimental test cross-sectional view as conducted by Neuberger and his co-researchers (Neuberger et al., 2009)

2. Method

AUTODYN 2D was used in this study to determine the effects of sphere-shaped TNT charge explosion against exposed circular surface of RHA plates (see Figures 1 and 2). Figure 2 shows the cross-sectional view of the experimental test as conducted by Neuberger and his co-researchers (Neuberger et al., 2009), where; 'W' is the weight of the TNT in kg, 'R' is the standoff distance i.e. the distance between the central point of the TNT and the top surface of the RHA plate, 't' is the thickness of the RHA plate, 'D' is the diameter of the RHA plate, ' δ_t ' is the first or maximum deflection experienced by the RHA plate and finally ' δ_f ' is the final deflection experienced by the RHA plate. The simulations' steps that will be presented in this section include geometric modelling of air, spherical TNT, exposed circular surface of RHA plate; meshing, assigning the appropriate material properties to the respective geometries, applying the relevant boundary conditions, selection of solvers, processing the analyses and obtaining the final results.

2.1 Geometrical Setup

The first step was to model air, RHA plate and the TNT spherical charge in AUTODYN 2D as shown in Figure 3. The three dimensional experimental set up apparatus as performed by Neuberger and his co-researchers (Neuberger et al., 2009) was modelled in two dimensional space in AUTODYN 2D by taking advantage of the axisymmetric modelling space that could give similar results as a three dimensional modelling space (rotated 360° along the horizontal x-axis) in AUTODYN 2D. This method was utilized in order to reduce the computational processing time. Figure 3 shows the position of air, TNT, RHA plate, clamped end of the RHA plate and gauge point of the RHA plate. The gauge point recorded the first and final deflections of the RHA plate due to blast loading from the TNT charge.

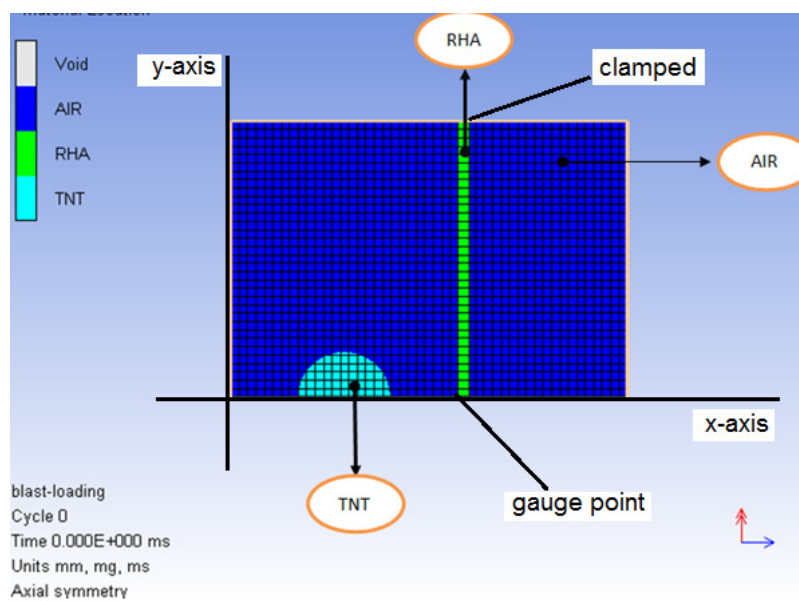


Figure 3. The numerical simulation model of air, TNT and RHA plate modelled in AUTODYN 2D

2.2 Element Meshing and Solvers

The materials used in this study comprised of air, TNT, RHA plate. The initial condition for the air was created. Square elements sizes of 5 mm x 5 mm were used for both of the air and RHA plate. The geometrical models were meshed with the appropriate number of elements in both 'x' and 'y' directions.

2.3 Properties of Air

The air and TNT gas product media were assumed to behave as an ideal gas, thus the default Equations of state (1), (2), (3) were specified. The air was specified with an internal energy of $2.068 \times 10^5 \text{ kJ kg}^{-1}$ in AUTODYN 2D.

$$P = \rho(\gamma - 1)E_0^a \quad (1)$$

$$\gamma = \frac{c_p}{c_v} \quad (2)$$

$$E_0^a = c_v T \quad (3)$$

where, 'ρ' is the density of gas, 'c_v' and 'c_p' are specific heats at constant volume and pressure, respectively; 'T' is the gas temperature, 'P' is the pressure, 'γ' is the ratio of specific heats and 'E₀^a' is the specific energy.

The air model was taken from AUTODYN 2D material library as shown in Table 2.

Table 2. AUTODYN 2D material properties for air (www.ansys.com)

ρ(kg/m ³)	T(K)	c _p (kJ/kg K)	c _v (kJ/kg K)
1.225	288.2	1.005	0.718

2.4 Radius of TNT Charge

Calculations for Case 'B' were performed and presented to determine the diameter of TNT from the data provided by AUTODYN 2D software. The density of TNT given by AUTODYN 2D is $\rho = 1.63 \frac{g}{cm^3}$ and Equation (4) gives

$$v = \frac{m}{\rho} \quad (4)$$

where, v is the volume of sphere-shaped TNT, m is the mass of TNT and ρ is the density of TNT. Then, the values of mass and density of TNT were substituted into Equation (4) to obtain its volume.

Hence, the volume of TNT obtained was $v = 5368.098 \text{ cm}^3$ for Case 'B'.

The radius of TNT for Case 'B' was calculated by using Equation (5).

$$r = \sqrt[3]{\frac{3v}{4\pi}} \quad (5)$$

Finally, the radius of sphere-shaped TNT that was modeled in AUTODYN 2D was $r = 10.862 \text{ cm}$ for Case 'B', similar steps were taken in order to calculate the TNT radii for Case 'A' and Case 'C', respectively.

2.5 Properties of the RHA Plate

In this study, the thickness of all three RHA steel plates used was 20 mm with 1 m in diameter. The yield stress of the RHA steel plate was 0.95 GPa (Neuberger et al., 2009). Neuberger and his co-researchers (Neuberger et al., 2009) stated that RHA steel plate was considered as a strain rate sensitive material and can be represented by the Johnson-Cook (J-C) constitutive model. The J-C model is as stated in Equation (6).

$$\sigma_y = (A + B \cdot \varepsilon_p^{-n}) \cdot (1 + c \cdot \ln \dot{\varepsilon}^*) \cdot (1 - T^m) \quad (6)$$

where 'A', 'B', 'c', 'n' and 'm' are the J-C material coefficients, 'ε_p' is the effective plastic strain, $\dot{\varepsilon}^* = \dot{\varepsilon}^{-p}/\dot{\varepsilon}_0$ is the effective plastic strain rate at a reference strain rate, $\dot{\varepsilon}_0 = 1 \text{ s}^{-1}$, and the homologous temperature

$T = (T' - T'_{\text{room}})/(T'_{\text{melt}} - T'_{\text{room}})$; where, T' is the material's temperature, T'_{room} is the room temperature, and T'_{melt} is the material's melting temperature.

2.6 Explosive TNT Model

The explosive TNT behavior was modeled by using the Jones-Wilkins-Lee (JWL) (Neuberger et al., 2009) equation stated in Equation (7) for a TNT explosive material as defined in the AUTODYN 2D material library. AUTODYN 2D will automatically revert to using the ideal-gas equation of state to handle the high pressure and temperature gases left after the explosion as soon as the TNT has completely detonated leaving only the gas products and surrounding air.

$$P = A \left(1 - \frac{\omega}{R_1 V}\right) e^{-R_1 V} + B \left(1 - \frac{w}{R_2 V}\right) e^{-R_2 V} + \frac{w E'}{V} \quad (7)$$

where, 'P' is pressure; 'A', 'B', 'C', 'R₁', 'R₂' and 'ω' are material constants that are empirically derived, $V = \frac{v}{v_0}$ is the relative volume of the gas products to the initial explosive state and E' is the energy per unit volume.

The LAGRANGE element formulation solver utilizes a mesh that moves and distorts with the material it models as a result of forces from neighboring elements (www.ansys.com). This is the most efficient solution methodology for solid with accurate pressure history definition. However, there is some limitation for LAGRANGE solver. If there is too much deformation of any element, it results in a very slowly advancing solution and is usually terminated because the smallest dimension of an element results in a time step that is below the threshold level. Hence, only the RHA plate was modeled using the LAGRANGE solver.

In contrast to the LAGRANGE solver, the EULER (multi-material) solver utilizes a fixed mesh, allowing materials to flow from one element to the next element (www.ansys.com). The EULER solver is more suitable for problems involving extreme material movement, such as fluids and gases. Hence, the air and TNT were modeled using EULER solver. However, EULER solver is generally more computationally intensive than LAGRANGE and requires higher resolution (smaller elements) to accurately capture sharp pressure peaks that often occur with shocks. The blast/explosion event was modeled using the EULER solver. The blast loading equation is stated in Equation (8) (Neuberger et al., 2009).

$$P(\tau) = P_r \times \cos^2 \theta + P_i \times (1 + \cos^2 \theta - 2 \cos \theta) \quad (8)$$

where, 'θ' is angle of incidence, 'P_r' is reflected pressure and 'P_i' is incident pressure.

2.7 Boundary Conditions

The next step was to define an outflow boundary condition for all three types of material. The plate was modelled using the LAGRANGE solver, while air and TNT were modelled using the EULER solvers. The outflow boundary condition was applied on the left side of the RHA plate where the TNT charge was located (see Figure 3). A boundary condition of 'x=0 and y=0 velocities' directions were applied to clamp one end of the RHA plate. The next step was to set up the interaction between TNT and RHA plate, where the EULER/LANGRANGE coupling type with 'Automatic' (polygon free) was utilised. Finally, the detonation of the explosive was set up by selecting the detonation point. This was followed by the setup solutions, output controls and the time limit of the explosion.

3. Results

Figures 4, 5 and 6 show the AUTODYN 2D numerical simulations' results after the TNT charge detonates for a time duration of about 30 milliseconds. The analyses were processed by using Intel(R) Core(TM) i5-3210M CPU @ 2.50 GHz, 4.0 GB, 32 bit operating system and took about 180 minutes to complete. All three figures consisted of three main materials' locations i.e. TNT, RHA plate and air. It could be observed that the TNT charge had fully detonated and filled the whole area of the left side of the RHA plate. The area on the right of the RHA plate was only occupied with air since the TNT explosion was restricted to the left side of the RHA plate. Meanwhile, the top part of the RHA plate remained at its original position because it was fully clamped in the 'x and y' directions representing the outer perimeter of the experimental RHA plate where it was fully constrained around its outer circular perimeter. The bottom part of the RHA showed maximum deflection due to its central position and it was located directly underneath the TNT charge. Simulation results were consistent with the final deflection results of the experimental results whereby the maximum deflection of the RHA plate occurred at the central part of the RHA plate.

Simulation also recorded the deflection of the central point of the RHA plate located directly to the right of the TNT charge as shown in Figures 7 and 8 for Case ‘B’. The first deflection was the maximum initial peak movement due to the direct blast loading effects from the explosion of the TNT charge (see Figure 7). After the RHA plate reached the maximum initial deflection, due to its elastic springback properties, the plate will continuously vibrate for quite some time. The final deflection of the RHA plate was taken based on getting an average value of amplitudes of the curve (see Figure 8). Table 3 shows the first and final deflections of the RHA plate as predicted by AUTODYN 2D for all three cases i.e. Case ‘A’, case ‘B’ and case ‘C’ were recorded and compared with respect to the experimental results of Neuberger and his co-researchers (Neuberger et al., 2009). It could be observed that the numerical simulation by AUTODYN 2D had managed to give good predictions against the experimental results (Neuberger et al., 2009) for both the first and final deflections.

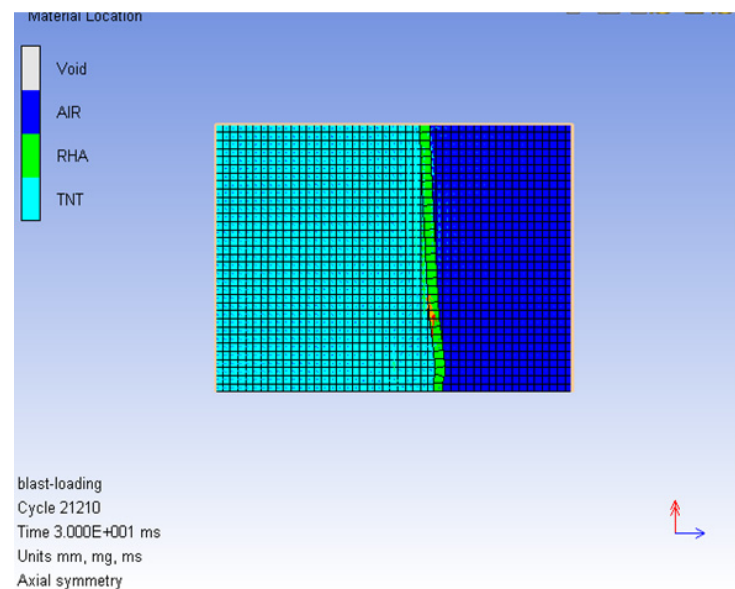


Figure 4. The final deflection of the AUTODYN 2D numerical simulation of the RHA plate (Case A) subjected to spherical TNT explosion

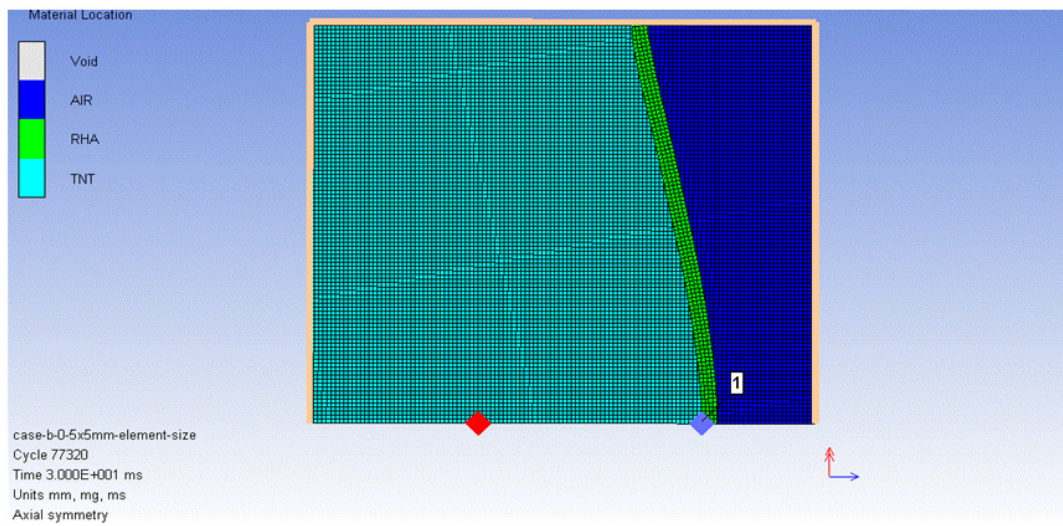


Figure 5. The final deflection of the AUTODYN 2D numerical simulation of the RHA plate (Case B) subjected to spherical TNT explosion

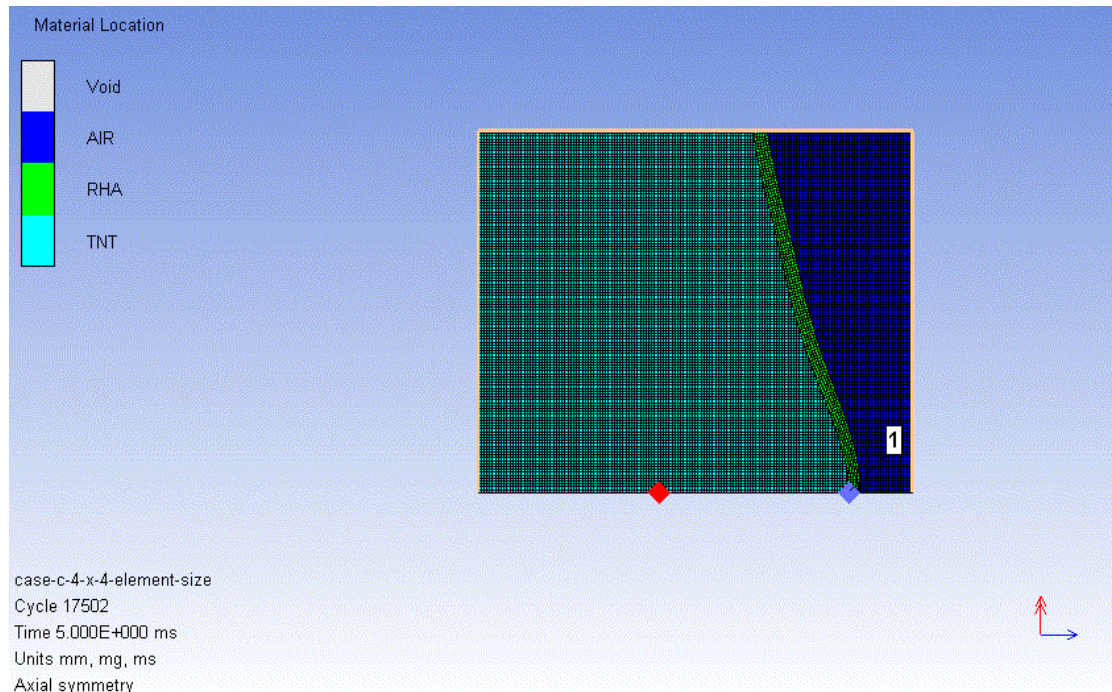


Figure 6. The final deflection of the AUTODYN 2D numerical simulation of the RHA plate (Case C) subjected to spherical TNT explosion

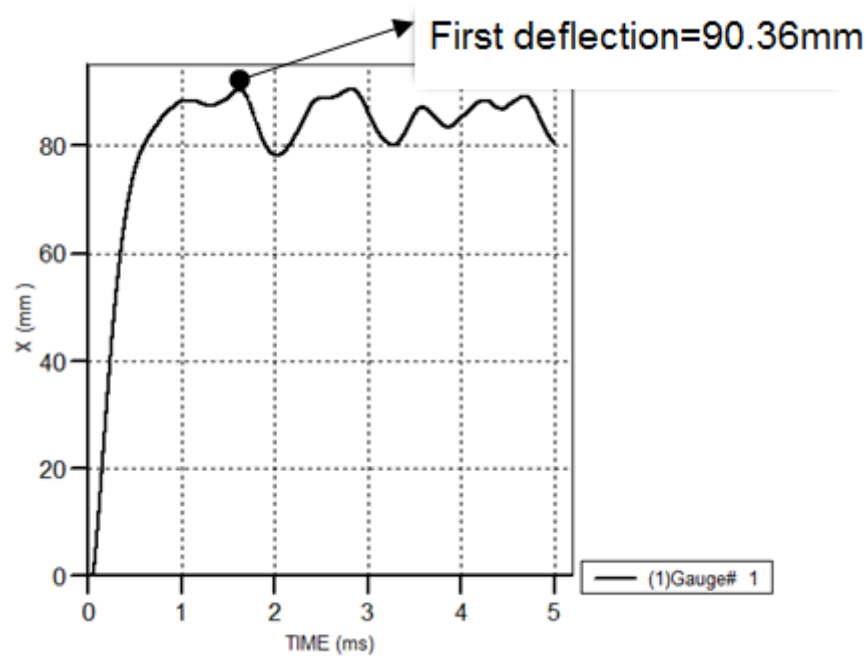


Figure 7. The first deflection of the numerical simulation of the RHA plate (Case B) subjected to spherical TNT explosion as predicted by AUTODYN 2D

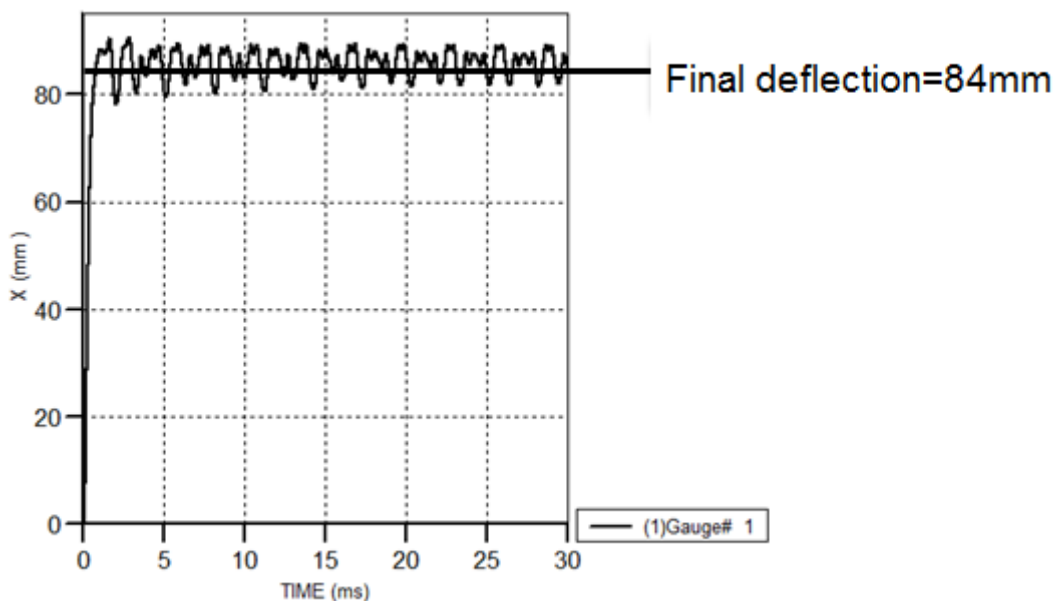


Figure 8. The final deflection of the numerical simulation of the RHA plate (Case B) subjected to spherical TNT explosion as predicted by AUTODYN 2D

Table 3. The first and final deflections of the RHA plate as predicted by the numerical simulation AUTODYN 2D compared against Neuberger and his co-researchers (Neuberger et al., 2009) experimental results

Case	Experimental test [8]; First deflection (mm)	AUTODYN 2D; First deflection (mm)	% differences	Experimental test [8]; Final deflection (mm)	AUTODYN 2D; Final deflection (mm)	% differences
'A'	54	43	20.37 %	7	6	14.28 %
'B'	107	90.36	15.55 %	64	84	31.25 %
'C'	165	138.06	16.32 %	121	133	9.91 %

4. Discussion

The results obtained from numerical analysis method using AUTODYN 2D were promising and compared favourably with the experimental results from Neuberger and his co-researchers (Neuberger et al., 2009). However, the numerical analysis method needs further refinements to reduce the differences between simulation and experimental results. By observing Case 'B' for example, AUTODYN 2D predicted the first deflection of 90.36 mm compared to the experimental result from Neuberger and his co-researchers (Neuberger et al., 2009) which was 107 mm (differences of 15.55 %) and AUTODYN 2D predicted the final deflection of 84 mm compared to the experimental result from Neuberger and his co-researchers (Neuberger et al., 2009) which was 64 mm (differences of 31.25 %). There were several reasons that contributed to first and final deflections' differences for all three cases.

There was a slight dissimilarity between the boundary condition applied in the numerical simulation and in the actual experimental tests as performed by Neuberger and his co-researchers (Neuberger et al., 2009). The circumference of the exposed circular surface of the RHA plate was not fully clamped during the experimental tests; instead, the original square shaped RHA plate was clamped in place by sandwiching the RHA plate in between two thick high strength steels and tightened by sets of bolts and nuts (see Figures 1 and 9). On the contrary, a fully clamped boundary condition was applied to the top portion of the RHA plate in the numerical simulation to hold the circumference of the RHA plate in place due to the two dimensional modeling space

limitations, thus the difference in setting the boundary conditions in the numerical simulation and the actual experimental tests will certainly produce slight errors between both methods.

Numerical analyses by utilizing finite element analysis software i.e. AUTODYN 2D have been performed to predict the deformation of exposed circular RHA plates due to TNT blast loadings. The two dimensional modeling space as utilized by AUTODYN 2D managed to give relatively good agreement against experimental results with differences of around 9.91%-31.25% and could be used as initial investigations to predict blast related problems. Further work is still needed in order to get more improved/accurate results, where AUTODYN 3D could be employed to model and analyze the problem in its actual three dimensional modeling space. In the three dimensional modeling space, AUTODYN 3D would be able to capture/model the full geometry of the RHA plate, the location of bolts, columns (see Figure 9), that would significantly improve the AUTODYN 2D results due to the limitations of boundary conditions encountered in the two dimensional modelling space.



Figure 9. The final geometry of the deformed RHA plate after the experimental blast test as performed by Neuberger and his co-researchers (Neuberger et al., 2009)

References

- Chafi, M. S., Karami, G., & Ziejewski, M. (2009). Numerical analysis of blast-induced wave propagation using FSI and ALE multi-material formulations. *International Journal of Impact Engineering*, 36, 1269-1275. <http://dx.doi.org/10.1016/j.ijimpeng.2009.03.007>
- Henchie, T. F., S. Chung, K. Y., Nurick, G. N., Ranwaha, N., & Balden, V. H. (2014). The response of circular plates to repeated uniform blast loads: An experimental and numerical study. *International Journal of Impact Engineering*, 74, 36-45, <http://dx.doi.org/10.1016/j.ijimpeng.2014.02.021>
- Huon, B., Paul, P., & Christopher, A. (2015). Evaluation of the blast mitigating effects of fluid containers, *International Journal of Impact Engineering*, 75, 222-228, <http://dx.doi.org/10.1016/j.ijimpeng.2014.08.014>
- Md Fuad, S. bin K., Ahmad, M. A. Z., Mohd, Z. O., Shohaimi, A., Suresh, T. (2013). The Effect of Mesh Sizing Toward Deformation Result in Computational Dynamic, Simulation for Blast Loading Application. *Modern Applied Science*, 7(7). <http://dx.doi.org/10.5539/mas.v7n7p23>
- Neuberger, A., Peles, S., & Rittel, D. (2009). Springback of circular clamped armor steel plates subjected to spherical air-blast loading. *International Journal of Impact Engineering*, 36, 53-60. <http://dx.doi.org/10.1016/j.ijimpeng.2008.04.008>
- New York Daily News (2014). Retrieved from www.nydailynews.com/news/national/boston-marathon-bomb-devices-made-pressure-cookers-filled-nails-b-all-bearings-report-article.1.1318278#ixzz2mheohvAC
- Schiffer, A., & Tagarielli, V. L. (2014). The dynamic response of composite plates to underwater blast: Theoretical and numerical modeling. *International Journal of Impact Engineering*, 70, 1-13.

- <http://dx.doi.org/10.1016/j.ijimpeng.2014.03.002>
- Smith, P. D., & Hetherington, J. G. (1994). *Blast and ballistic loading of structures*. Butterworth-Heinemann Ltd, United Kingdom.
- Subramaniam, K. V., Nian, W., & Andreopoulos, Y. (2009). Blast response simulation of an elastic structure: Evaluation of the fluid-structure interaction effect. *International Journal of Impact Engineering*, 36, 965-974. <http://dx.doi.org/10.1016/j.ijimpeng.2009.01.001>
- Xiang, F., Dong, L., & Lijun, X. (2011). A Composite Detection and Disposal Scheme for Explosive Embedded in Building. *Modern Applied Science*, 5(3). <http://dx.doi.org/10.5539/mas.v5n3p136>
- Yaohua, W., Liang, W., Xiaoqiang, Y., Baoguo, Z., Haishan, Y., & Yunfeng, W. (2011). The Security Quantitative Analysis Model of EED Based on Burning and Explosion Dangerous Source Evaluation Method. *Modern Applied Science*, 5(4). <http://dx.doi.org/10.5539/mas.v5n4p112>

Copyrights

Copyright for this article is retained by the author(s), with first publication rights granted to the journal. This is an open-access article distributed under the terms and conditions of the Creative Commons Attribution license (<http://creativecommons.org/licenses/by/3.0/>).